

Supplement of Biogeosciences, 15, 5015–5030, 2018  
<https://doi.org/10.5194/bg-15-5015-2018-supplement>  
© Author(s) 2018. This work is distributed under  
the Creative Commons Attribution 4.0 License.



*Supplement of*

## **Basic and extensible post-processing of eddy covariance flux data with REddyProc**

**Thomas Wutzler et al.**

*Correspondence to:* Thomas Wutzler ([twutz@bgc-jena.mpg.de](mailto:twutz@bgc-jena.mpg.de))

The copyright of individual parts of the supplement might differ from the CC BY 4.0 License.

## 1 Details of marginal distribution sampling (MDS) for gap-filling

The marginal distribution (section 2.2.3) combines the two methods look-up-table (LUT) and mean diurnal course (MDC). Depending on the availability of the meteorological data, three different conditions are identified for each half-hourly NEE flux:

1. The data of the three meteorological variables (Rg, Tair, and VPD) are available.
2. Tair or VPD are missing, but Rg is available.
3. Also Rg is missing.

Case 1): The missing value is replaced by the average value under similar meteorological conditions with respect to Rg, Tair and VPD in a LUT approach. If no similar meteorological conditions (minimum of two half-hourly fluxes) are present within the starting time window of 7 days, the window size is increased to 14 days.

Case 2): The same LUT approach is taken, but similar meteorological conditions can only be defined via Rg within a time window of 7 days.

Case 3): The missing value is replaced with the mean diurnal course (MDC). The number of days start with one day, thus a linear interpolation of available data at adjacent hours ( $\pm 1$  hour) at the same day. The number is then increased to  $\pm 1$  and  $\pm 2$  days.

If after these steps the NEE values could not be filled, the procedure is repeated with increased window sizes until the value can be filled, see flow diagram in Fig. 1.

The provided quality flag depends on both, the number of meteorological conditions present,  $n_c$ , and the number of days in the window,  $n_d$ . When using LUT, the flag equals 1 when  $n_c$  is either 1 or 3 and  $n_d \leq 7$ . It equals 3 if either  $n_c = 3$  and  $n_d > 28$ , or  $n_c = 1$  and  $n_d > 14$ . In all other LUT cases, it equals 2. When using MDC, i.e.  $n_c = 0$ , the quality flag equals 1 if it is the same day, it equals 3 if  $n_d > 2$ , and it equals 2 in all other cases.

The three default variables and margins are Rg with  $\pm 50$   $\text{Wm}^{-2}$ , Tair with  $\pm 2.5$   $^\circ\text{C}$ , and VPD with  $\pm 5.0$  hPa. These can be also be specified by the user.

## 2 Details of daytime flux-partitioning

This section reports details of the steps for daytime flux-partitioning (section 2.3.2).

In step 1, parameter  $E_0$  is estimated for 12 day windows. Only records with temperature above  $-1$   $^\circ\text{C}$  are valid for estimation. Reference temperature  $T_{Ref}$  in eq. 1 of the paper is set to the median temperature of the window in order to decrease correlation between estimates of  $R_{Ref}$  and  $E_0$ . A missing estimate is reported for non-valid windows with too few valid records ( $\text{minNRecInDayWindow} = 10$ ), non-convergence of the fitting procedure, or an  $E_0$  estimate outside the bounds [50,400]. Missing estimates are filled during the smoothing in step 2.

In step 2, the Gaussian Process takes into account the uncertainty of the  $E_0$  fit from night-time in each window. However, if the correlation of  $E_0$  across subsequent windows is high, the uncertainty is reduced similar as with repeated measurements. The respiration  $R_{Ref}$  for windows where no fit could be obtained is set to the value from the previous valid window. Again, only records with temperature above  $-1$   $^\circ\text{C}$  are used.

In step 3, fitting of other parameters is done for each window centered at the same record as the windows of step 1. By default the fit uses the same weak prior on parameters as BGC16 (Lasslop et al., 2010). The optimization minimizes a cost function using the "BFGS" method, which is a quasi-Newton method as published by Shanno (1970). The cost function assumes normally distributed model-data-residuals and normally distributed vague priors (eq. 1) (Lasslop et al., 2010, eq. 5).

$$c = \sum_i \frac{(NEE_{pred,i} - NEE_{obs,i})^2}{\sigma_{NEEadj,i}^2} + \sum_j \frac{(\theta_j - \theta_{prior,j})^2}{\sigma_{\theta,j}^2}, \quad (1)$$

where  $NEE_{pred,i}$  is computed by the LRC equation, and parameters  $\theta = (k, \alpha, R_{Ref}, \beta)$  have prior locations of  $k = 0.05$ ,  $\alpha = 0.1$ ,  $R_{Ref}$  = night-time estimate, and  $\beta$  = range of NEE values, i.e. the difference between 97% and 3% quantile. The prior uncertainty is  $\sigma_k = 50$ ,  $\sigma_\beta = 600$ ,  $\sigma_\alpha = 10$ , and  $\sigma_{R_{Ref}} = 80$ .

The uncertainty of NEE by default is assigned a lower bound (eq. 1). This lower bound differs from Lasslop et al. (2010) and assigns low influence to records with high uncertainty in order to avoid the problem of high leverage of a few records with very low estimates of NEE-uncertainty.

$$\sigma_{NEEadj,i}^2 = \max[\sigma_{NEE,i}^2, q_{0.3}(\sigma_{NEE}^2)], \quad (2)$$

where  $q_{0.3}(\sigma_{NEE}^2)$  is the 30% quantile of the vector of estimated standard deviations of NEE.

There are several quality criteria and fall-backs during the daytime fitting in order to obtain reasonable fits. If there are too few valid records ( $\text{minNRecInDayWindow} < 10$ ), or the

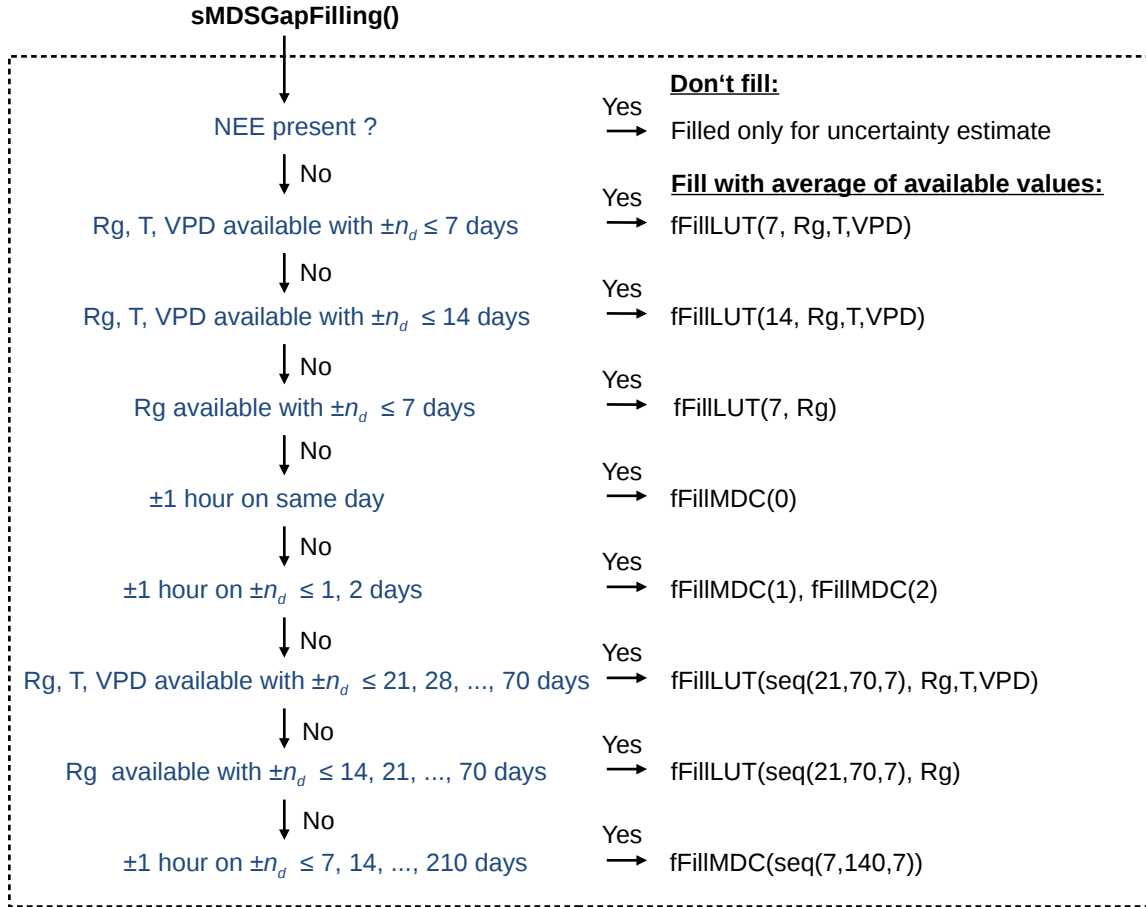


**Figure 1.** Flow diagram of the MDS gap-filling algorithm as implemented in REddyProc. See table 1 in the main paper for abbreviations.

fitting did not converge, or VPD parameter  $k < 0$ , then the fit is repeated without the VPD effect, because often there are records where VPD is missing but other variables are available. If fitting did not converge or parameter estimate of  $\alpha$  is larger than 0.22, the fit is repeated with  $\alpha$  fixed to the last valid value of  $\alpha$  from fits in previous windows. If there are still too few records or the fitting was not valid, a missing result is reported for the window. In addition a missing result is reported if estimated  $\alpha < 0$  or  $R_{Ref} < 0$  or  $\beta_0 < 0$  or  $\beta_0 > 250$ , or if  $\beta_0 > 100$  and at the same time estimated standard deviation  $sd_{\beta_0} \geq \beta_0$  (Table A1 in Lasslop et al., 2010). The Variance-Covariance matrix of the parameter uncertainty is estimated by bootstrapping the day-time fit. In each sample, the prescribed temperature sensitivity  $E_0$  is drawn from a normal distribution with standard deviation estimated in step 2. In this way also the uncertainty of the night-time fit propagates to the uncertainty of the day-time parameters and subsequently to the inferred gross fluxes.

In step 4, variance of the flux estimates are computed based on the Variance-Contrivance matrices obtained in step 3 with

each parameter estimate (Lasslop et al., 2010, eq. 6). The two standard deviations based either on the previous and subsequent valid estimates of the Variance-Contrivance matrices are linearly interpolated with respect to the time difference to the estimates.

### 3 General design of REddyProc

There are some general principles and choices in the design of REddyProc which may lead to some trade-offs.

**Preventing accidental errors** is one goal of the package. Therefore, there is extensive checking on formatting and data availability when importing the data and also throughout post-processing steps. Especially, the high-level routines will issue warnings or stop post-processing if they detect inconsistencies or lack of sufficient data, or changes in specification of critical standard parameters. These checks reinforce a sound standard post-processing also for non-expert users. On the other hand, these checks will render the standard routines not usable for

datasets where not enough data are available. It is still possible to use REddyProc with sparse data for some purposes by using lower-level routines. But this requires experience in both, post-processing and R programming.

5 **Smooth inter-annual processing** is the next goal. The data is not partitioned into annual chunks for post-processing to avoid artificial discontinuities between years. The user can still specify different periods or seasons, e.g. when meteorological conditions change after harvest, but the boundaries do not  
 10 need to align with years. REddyProc therefore works with the entire dataset in memory. Potentially this can lead to longer post-processing times when working with many years of EC data but still can be handled on a usual notebook.

**Memory efficient processing** required some extended R programming. Specifically we used R5 classes<sup>1</sup> to avoid frequently copying the entire dataset in memory. Users should be aware that calling functions on the sEddyProc class not only provides a return value but also changes the data of the R5 class (Chapter 'OO field guide' in Wickham, 2014). Users  
 20 who want to integrate the post-processing in their own codes are encouraged to learn about R5 classes, however, it is not a prerequisite.

**Continuity with other tools** ensures that switching to REddyProc does not introduce discontinuities with results  
 25 obtained from other tools. Specifically, we reproduced the  $u_*$  threshold estimation of the C implementation by Dario Papale (DP06), and the gap-filling, night-time flux partitioning, and day-time flux-partitioning from BGC16, the 2016 version of the BGC online tool (Reichstein et al., 2005). In some details,  
 30 the standard parameterization differs from BGC16, e.g. using seasons that span across calendar years in  $u_*$  threshold estimation, but it is usually possible to set compatible parameters with REddyProc.

#### 4 Additional benchmark statistics

35 This section provides figures, in addition to the main figures presented in the paper's benchmark section, that require the reader being comfortable with histograms and probability distribution functions.

The histograms display how often a certain value occurs  
 40 across all the site-months. A centering of a difference away from zero or for a ratio away from one denotes a bias.

##### 4.1 $u_*$ threshold estimation

There was a bias in  $u_*$  estimation compared to DP06 (Fig. 2). However, the bias and the differences were only a small

<sup>1</sup> [www.rdocumentation.org/packages/methods/versions/3.4.3/topics/ReferenceClasses](http://www.rdocumentation.org/packages/methods/versions/3.4.3/topics/ReferenceClasses)

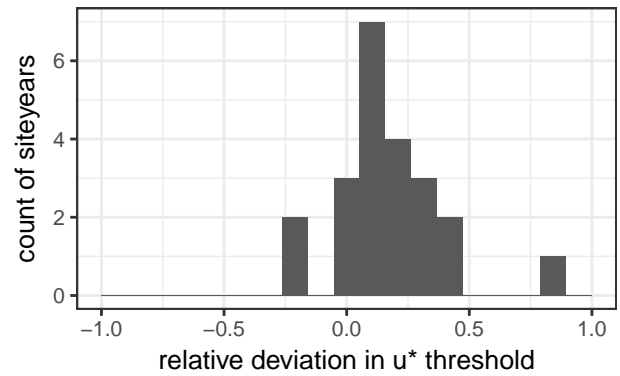


**Figure 2.** Histogram of differences between  $u_*$  threshold estimates of different methods (DP06 - REddyProc) normalized by the uncertainty range (90% quantile - 10% quantile estimated by DP06). Absolute values are smaller than one meaning that the difference between the methods is smaller than range of estimates by the DP06 method only. The clustering of values on the positive side suggests a bias towards larger values with DP06.

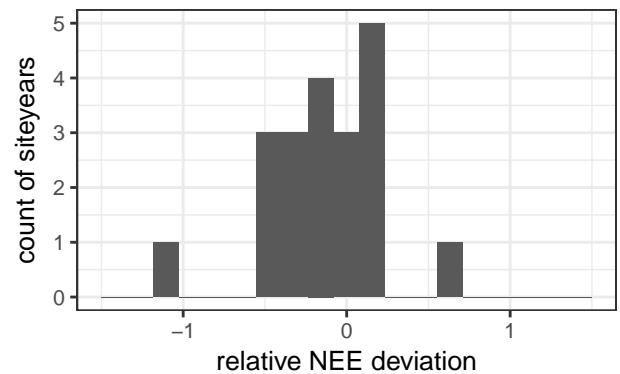


**Figure 3.** Histogram of differences between annual NEE based on  $u_*$  estimates of different methods (DP06 - REddyProc) normalized by the uncertainty range of NEE due to  $u_*$  (NEE based on 90%  $u_*$  quantile - NEE based on 10%  $u_*$  quantile estimated by DP06). Absolute values are mostly smaller than one, meaning that the difference in annual NEE between methods is smaller than the uncertainty due to uncertainty of  $u_*$  threshold from DP06 only.

fraction of the uncertainty of the estimate itself. Moreover, the  
 45 bias did not propagate to estimated NEE based on different  $u_*$  values (Fig. 3).

There was a significant difference in the estimate of uncertainty of the  $u_*$  thresholds (Fig. 4). The uncertainty estimated by REddyProc was only half as high as the one estimated  
 50 by DP06. It resulted from acknowledging the seasons of similar conditions also during bootstrap. The lower  $u_*$  threshold uncertainty propagated to the uncertainty estimates of NEE (Fig. 5).

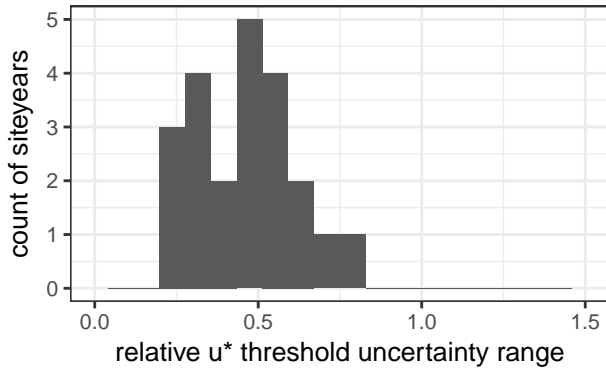


**Figure 4.** Histogram of ratio ( $\text{REddyProc} / \text{DP06}$ ) of uncertainty ranges of  $u_*$  (90% quantile - 10% quantile). The clustering around 0.5 shows that the estimated uncertainty with  $\text{REddyProc}$  is only about half the uncertainty estimated by  $\text{DP06}$ .

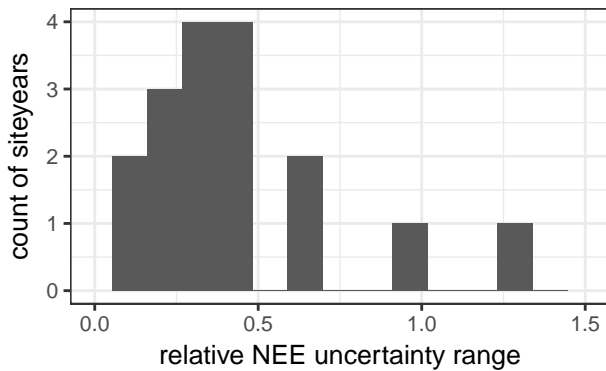


**Figure 5.** Histogram of ratio ( $\text{REddyProc} / \text{DP06}$ ) of uncertainty ranges of annual NEE (NEE based on 90% quantile of  $u_*$  threshold - NEE based on 10% quantile of  $u_*$  threshold). The clustering below a value of one indicates that the lower uncertainty in  $u_*$  threshold with  $\text{REddyProc}$  also propagates to lower uncertainty in annual NEE.

## 4.2 Gap-filling

The evaluation of annual aggregated NEE data obtained with  $\text{REddyProc}$  and  $\text{BGC16}$  showed good agreement across sites.

- 5 Note, that the aggregated NEE data contained both, measured and gap-filled data for the purpose of evaluating the impact of the processing on the aggregated NEE. The determination coefficient ( $R^2$ ) showed a very good agreement between the two methods both at annual and monthly time scale (Table 1).  
 10 The relative mean absolute error (RMAE) is low: about -3 % for annual aggregation and -0.47 % for monthly aggregation. Both Modeling Efficiency (EF) and Mean Bias Error (MBE) showed a very low bias between the two products for both monthly and annual aggregations (Table 1).

**Table 1.** Gap-filling evaluation statistics of yearly and monthly cumulated and gap-filled NEE data obtained with  $\text{REddyProc}$  and  $\text{BGC16}$ . Statistic abbreviations are explained in the paper's benchmarking section

	Yearly	Monthly
N	25	281
pearson	0.99	1.00
MBE	-0.02	0.00
RMBE	2.8%	-0.08%
MAE	0.02	0.00
RMAE	-3.0%	-0.5%
RMSE	0.09	0.01
$R^2$	0.98	1.00
EF	0.98	1.00

## 4.3 Night-time partitioning

15

The results show good agreement between  $R_{\text{eco}}$  estimated using  $\text{REddyProc}$  and  $\text{BGC16}$  for  $R^2$  and modelling efficiency (Table 2). The relative RMSE is 6.56 and 13.45 % for yearly and monthly aggregation, respectively. The high RRMSE is due to few site years as reported in Table 3, and this is confirmed by the lower RMAE (3.87 % and 6.33 % for yearly and monthly, respectively), which is less sensitive to outliers.

20

The difference in  $R_{\text{eco}}$  related to the selection of night-time data are not negligible: the differences in RRMSE of 1.03% and negligible differences in  $R^2$ . Also, the use of  $E_0$  prescribed from  $\text{BGC16}$  lead to negligible difference in  $R^2$  of about 0.02. Therefore, though very small, the selection of night-time data is the most important difference introduced by  $\text{REddyProc}$ .

25

30

**Table 2.** Nighttime partitioning evaluation statistics across sites of annually and monthly aggregated ecosystem respiration ( $R_{\text{eco}}$ ) estimated with  $\text{REddyProc}$  and  $\text{BGC16}$ .

	Yearly	Monthly
N	25	297
pearson	0.99	0.99
MBE	25.4	2.15
RMBE	2.2%	2.2%
MAE	44.8	6.17
RMAE	3.8%	6.3%
RMSE	75.6	13.2
RRMSE	6.5%	13.5%
$R^2$	0.99	0.98
EF	0.99	0.97

## 4.4 Day-time partitioning

The time-variable estimate of temperature sensitivity of ecosystem respiration with day-time partitioning is a signif-

	RMBE	RMAE	RRMSE	$R^2$	EF
CA-NS7	15.12	16.29	32.64	0.96	0.86
CA-TP3	-1.99	25.10	38.59	0.87	0.82
DE-Hai	6.00	6.48	10.40	0.99	0.96
DE-Tha	2.83	3.52	6.19	0.99	0.99
DK-Sor	3.50	4.45	7.34	1.00	0.99
ES-ES1	1.68	3.34	4.59	0.93	0.92
ES-VDA	3.96	9.98	15.93	0.95	0.93
FI-Hyy	2.72	3.05	4.47	1.00	1.00
FI-Kaa	-4.52	5.51	9.07	0.99	0.99
FR-Gri	3.96	4.14	6.35	1.00	0.99
FR-Hes	4.11	5.06	9.06	0.99	0.99
FR-Lq1	-2.89	5.76	7.24	0.99	0.99
FR-Lq2	-8.27	9.49	11.49	0.99	0.97
FR-Pue	0.65	1.27	1.55	1.00	1.00
IE-Dri	-0.03	2.41	3.24	1.00	1.00
IL-Yat	1.66	2.89	3.72	0.99	0.99
IT-Amp	24.34	29.38	45.33	0.91	0.48
IT-MBo	2.03	3.00	4.49	1.00	1.00
IT-SRo	-1.46	1.86	2.10	1.00	0.99
PT-Esp	9.06	12.08	19.94	0.62	0.45
RU-Cok	-0.76	28.54	38.98	0.27	-0.07
SE-Nor	-1.05	2.09	3.62	1.00	1.00
US-Ton	2.93	7.45	11.82	0.93	0.92
VU-Coc	0.73	2.64	3.83	0.93	0.93

**Table 3.** Nighttime partitioning evaluation statistics at sites level of the of ecosystem respiration ( $R_{eco}$ ) estimated with REddyProc and BGC16.

icant source of uncertainty for gross fluxes GPP and  $R_{eco}$ . REddyProc accounts for the previously unaccounted uncertainty for estimating uncertainty of these gross fluxes by a bootstrap (Fig. 6). The BGC16 estimate of annual uncertainty in Fig. 6 is a low estimate compared to a full quantification, because it assumes no correlation between half-hourly errors. An improved quantification of correlations requires the full variance-covariance matrix of the LRC parameter fits (Lasslop et al., 2010; Menzer et al., 2013), which were not available for BGC16.

The introduced uncertainty is reduced by smoothing the temperature sensitivity estimates ( $E_0$ ) across several successive windows (Fig. 7 top) before estimating parameters of the LRC. This smoothing has also an effect on predicted half-hourly gross fluxes (Fig. 7 bottom).

Results of daytime partitioning are sensitive to subtle details of the procedure. Hence, there is quite much scatter introduced by the differences of REddyProc processing with default options or with options that maximize compatibility with BGC16 (Fig. 8 top). One such a subtle options is to decrease or not to account for the unreasonably high leverage of some observations during the fit to the light-response curve by some records having a very small estimate of its uncertainty (Fig. 8 bottom). Due to the sensitivities of the day-time parti-

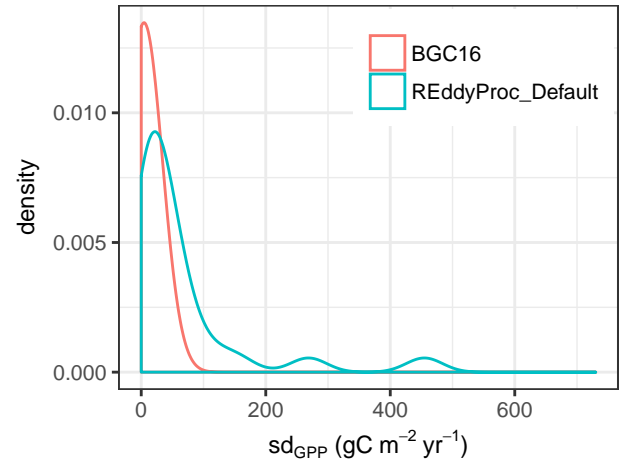


**Figure 6.** Density plot of estimated standard deviation of uncertainty of the annually aggregated GPP across sites due to uncertainty in parameters estimation during day-time based flux partitioning. Higher estimates with REddyProc are caused by taking into account the uncertainty in temperature sensitivity,  $E_0$ .

tioning, there are still differences between REddyProc with compatibility options and BGC16 (Fig. 9).

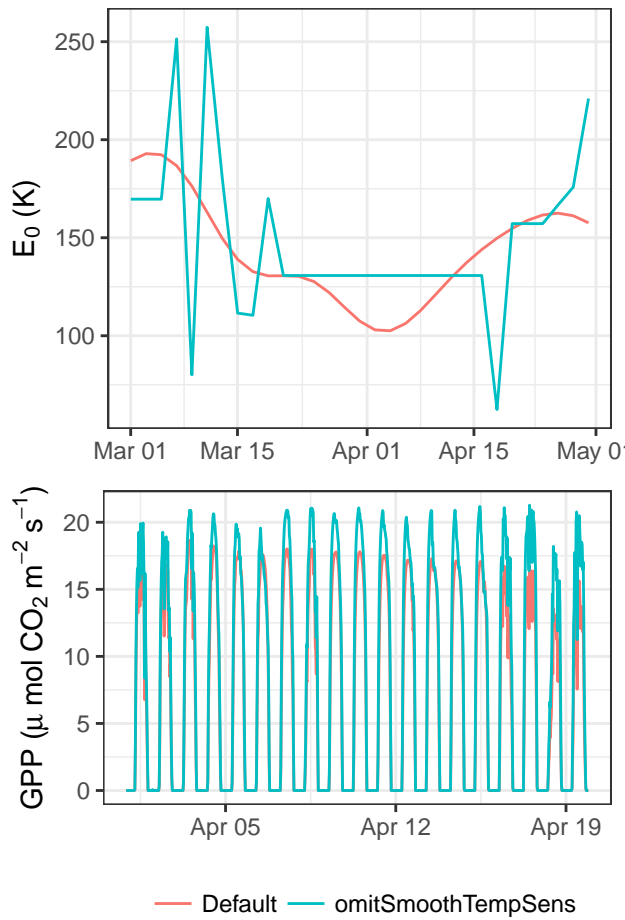


**Figure 7.** Effects of smoothing (top) successive estimates of temperature sensitivity,  $E_0$ , on predicted GPP (bottom) for site PT-Esp.

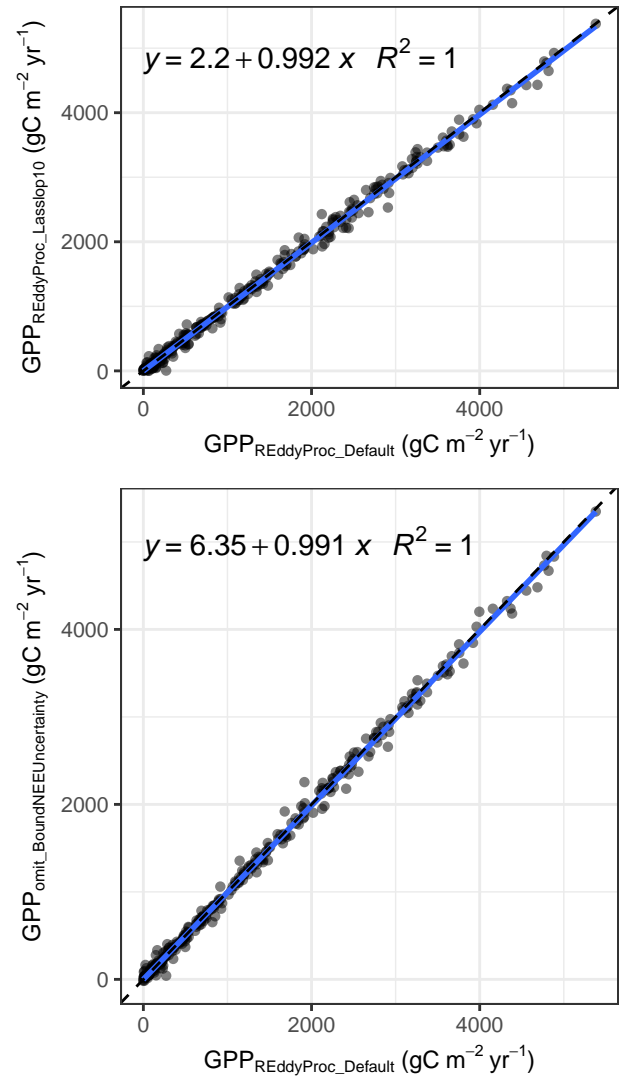


**Figure 8.** Sensitivity of estimated monthly GPP fluxes to specific processing details results in scatter between GPP predictions based on different REddyProc options. Most of the differences between default options and compatibility options (top) are caused by differences in weighting different records during the fit (bottom.)

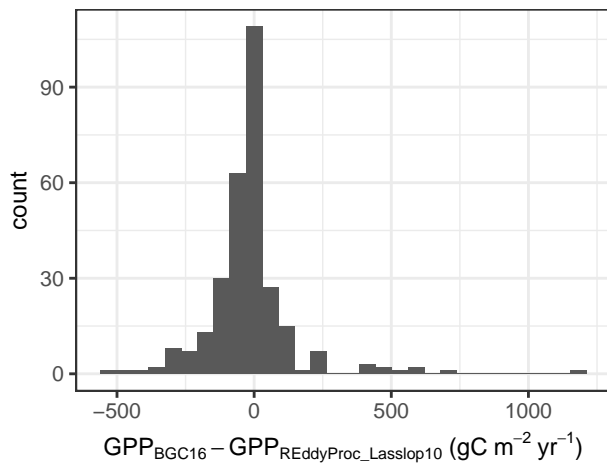


**Figure 9.** Histogram of difference between monthly GPP predictions of REddyProc with Lasslop10 compatibility options BGC16.



## References

- Lasslop, G., Reichstein, M., Papale, D., Richardson, A., Arneeth, A., Barr, A., Stoy, P., and Wohlfahrt, G.: Separation of net ecosystem exchange into assimilation and respiration using a light response curve approach: critical issues and global evaluation, *Global Change Biology*, 16, 187–208, <https://doi.org/10.1111/j.1365-2486.2009.02041.x>, 2010.
- Menzer, O., Moffat, A. M., Meiring, W., Lasslop, G., Schukat-Talamazzini, E. G., and Reichstein, M.: Random errors in carbon and water vapor fluxes assessed with Gaussian Processes, *Agricultural and Forest Meteorology*, 178-179, 161–172, <https://doi.org/10.1016/j.agrformet.2013.04.024>, 2013.
- Reichstein, M., Falge, E., Baldocchi, D., Papale, D., Aubinet, M., Berbigier, P., Bernhofer, C., Buchmann, N., Gilmanov, T., Granier, A., et al.: On the separation of net ecosystem exchange into assimilation and ecosystem respiration: review and improved algorithm, *Global Change Biology*, 11, 1424–1439, <https://doi.org/10.1111/j.1365-2486.2005.001002.x>, 2005.
- Shanno, D. F.: Conditioning of quasi-Newton methods for function minimization, *Mathematics of Computation*, 24, 647–647, <https://doi.org/10.1090/s0025-5718-1970-0274029-x>, 1970.
- Wickham, H.: *Advanced R*, Taylor & Francis Inc, 2014.